

# Convection in a partially molten metasedimentary crust? Insights from the El Oro complex (Ecuador)

Nicolas Riel<sup>1</sup>, Jonathan Mercier<sup>2</sup>, and Roberto Weinberg<sup>3</sup>

<sup>1</sup>Department of Earth Sciences, Durham University, Science Labs, Durham DH1 3LE, UK

<sup>2</sup>ISterre, University Grenoble I, CNRS-IRD, 1381 rue de la Piscine, BP53, 38041 Grenoble, France

<sup>3</sup>School of Earth, Atmosphere & Environment, Monash University, Clayton, 3800 VIC, Australia

## ABSTRACT

The El Oro complex, southwestern Ecuador, is a tilted section of the metasedimentary Ecuadorian forearc, which was partially molten during Triassic time due to gabbroic magma emplacement. Pressure and maximum temperature estimates show that the metamorphic gradient during anatexis was 45 °C/km in the upper crust and 10 °C/km in the 7–8 km garnet-bearing migmatitic lower crust, controlled by biotite-breakdown melting reactions. Our petrological and geochemical studies indicate that melts produced during biotite-breakdown (5–15 vol%) were trapped and pervasively distributed in the garnet-bearing migmatite. Based on these results we carried out one-dimensional thermal modeling to characterize the heat transfer processes that led to the establishment of such a low thermal gradient during partial melting. Our results show that neither diffusive nor upward melt transfer models account for the low metamorphic gradient in the garnet-bearing migmatite. We demonstrate that in the El Oro complex, convection of the garnet-bearing migmatitic layer is the most likely heat transfer process that explains all the petrological, geochemical, and metamorphic data.

## INTRODUCTION

Both the largest Himalayan-Tibet and the Altiplano-Puna orogenic systems exhibit multiple evidence of ongoing partial melting in the middle to lower crust (e.g., Caldwell et al., 2009; Yuan et al., 2000). The genesis and rheology of such high-temperature middle to lower crustal sequences are therefore key to better understand the evolution of large orogenic systems. Because well-preserved deep sections of the crust are rarely exposed, and commonly exhibit multiple events of partial melting, most of the data from these zones are based on chemical investigation of outcrops of volcanic and shallow plutonic bodies (e.g., Mahéo et al., 2009), numerical modeling (e.g., Bittner and Schmelting, 1995), metamorphic studies of xenoliths (e.g., Ding et al., 2007), or Rayleigh wave dispersion studies (e.g., Caldwell et al., 2009). However, such sections are exposed in some key areas where they may be investigated. The El Oro complex, located in southwestern Ecuador (Fig. 1A), is a well-preserved crustal section that underwent a single event of mafic magma underplating and consequent crustal melting (Riel et al., 2013). To study the thermochemical evolution of the El Oro complex during partial melting, we used (1) structural, petrological, and geochemical tools to characterize the chemical exchanges in the crust; (2) available and new pressure and maximum temperature estimates ( $P$ - $T_{\max}$ ); and (3) thermal modeling using previous results to constrain the heat transfer mechanisms and their rheological implications. Our study suggests that in the middle crust, whole-rock convection with low melt content (5–15 vol%) might occur during biotite-breakdown melting reactions at 780–900 °C. This can potentially account for

the formation of large volumes of partially molten middle crust in large orogenic systems.

Field photographs and detailed methodology for  $P$ - $T_{\max}$  estimates and geochemical and thermal modeling are provided in the GSA Data Repository<sup>1</sup>.

## GEOLOGICAL SETTING

The El Oro complex is a tilted forearc section composed of unmetamorphosed pelites and sandstones to the south that progressively grade to a migmatitic series to the north, juxtaposed northward by a gabbroic pluton and a blueschist unit (Fig. 1B). Both metamorphic and magmatic events, which include gabbro and the granitoid emplacement, occurred in the Late Triassic between 230 and 225 Ma (Riel et al., 2013). The intrusion of mid-oceanic ridge basalt-type gabbro at the crustal root level triggered partial melting of the overlying metasedimentary sequence and emplacement of the granitoid belt in the unmolten metasedimentary upper crust (Fig. 2). Tectonic underplating of the blueschist unit at  $226 \pm 1.8$  Ma (Gabriele, 2002) rapidly cooled both the gabbro pluton and the crust and marked the end of the anatectic event, allowing preservation of rare structures.

The granitoid belt that intrudes the unmolten metasedimentary unit is 1–2 km thick and composed of amphibole + biotite granodiorite and muscovite + biotite monzogranite with numer-

<sup>1</sup>GSA Data Repository item 2016008, photographs of the petrological study, geochemical methods, and detailed thermal and thermodynamic modeling methods, is available online at [www.geosociety.org/pubs/ft2016.htm](http://www.geosociety.org/pubs/ft2016.htm), or on request from [editing@geosociety.org](mailto:editing@geosociety.org) or Documents Secretary, GSA, P.O. Box 9140, Boulder, CO 80301, USA.

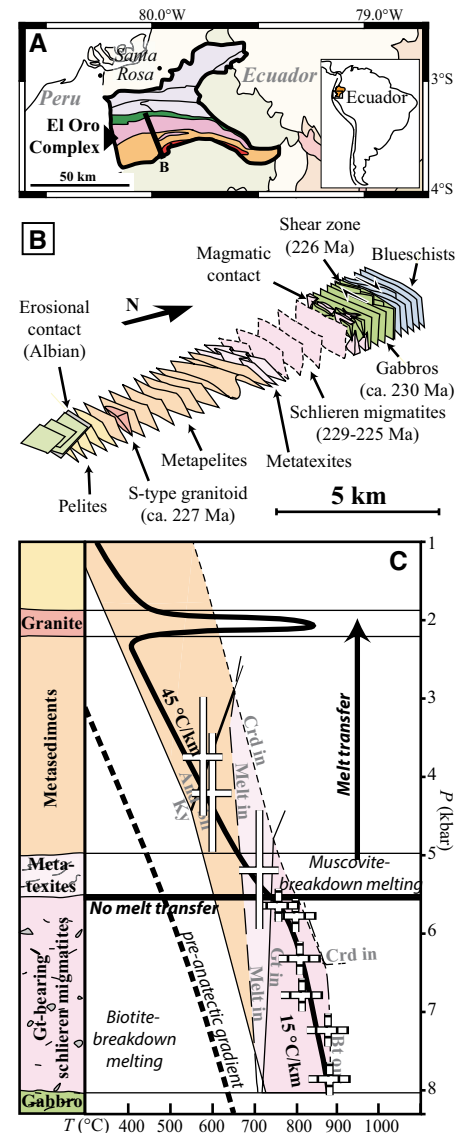


**Figure 1.** Geological features of the El Oro metamorphic province (southwestern Ecuador). Color legend in A is described in B. A: Simplified geological map of southwestern Ecuador. B: Geological cross section of the El Oro complex. C: Pressure-temperature profile with  $P$ - $T_{\max}$  estimates modified after Riel et al. (2013) (see the Data Repository [see footnote 1]). Fields where biotite (Bt) and muscovite breakdown reactions occur are indicated (Gt—garnet; Crd—corderite; Ky—kyanite; And—andalusite; Sil—sillimanite). A simplified geological log of the complex is shown on the left. Pressure estimates are extrapolated from the metatexite (sample PU0806; Riel et al., 2013) to the bottom of the La Bocana unit as a function of horizontal distance assuming that the sequence tilted 90°.

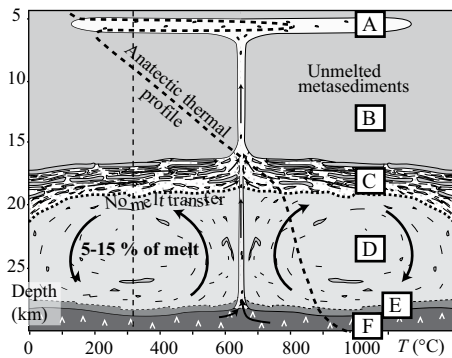


**Figure 2.** Interpretative model of the El Oro complex (southwestern Ecuador) after gabbro emplacement in the Triassic. **A**—S-type plutonic belt made of the mixing between muscovite-breakdown melts and gabbroic magmas; **B**—unmelted metasedimentary unit; **C**—muscovite-breakdown melting zone at 650–760 °C (metatexite); **D**—biotite-breakdown melting zone (schlieren migmatites) undergoing convection at 760–900 °C (garnet-bearing schlieren migmatites); **E**—mixing zone between crustal and gabbroic magmas; **F**—gabbro.

ous mafic enclaves. The metasedimentary unit is composed of metapelites and quartzites without evidence of dike intrusions (Riel et al., 2013). The migmatitic unit underlying these rocks has a quartzopelitic protolith and is lithologically divided into two parts. Partial melting in the upper, 1–2-km-thick metatexite, characterized by a stromatolitic leucosome, was controlled by muscovite-breakdown melting. In the lower garnet-bearing, 7–8-km-thick, mesocratic schlieren migmatite, partial melting was controlled by biotite-breakdown melting and contact with the underlying gabbro (Fig. 2) (Riel et al., 2013). The  $P$ - $T_{\max}$  estimates show that partial melting occurred between 650 °C and 760 ± 50 °C at 5–5.5 ± 2 kbar in the metatexites, and between 760 °C and 880 ± 50 °C at 5.5–8 ± 2 kbar in the schlieren migmatites (Riel et al., 2013; this study). The inferred metamorphic gradient exhibits a sharp change from a high of 45 °C/km in the upper crust to a low of 10–15 °C/km in the 7–8-km-thick schlieren migmatites (Fig. 1C). The bend point corresponds to the change in melting reactions from muscovite to biotite-breakdown melting (700–760 °C). Such a low geothermal gradient in the lower part of the system indicates heat advection, either by pervasive melt flow or whole-rock flow.

## STRUCTURE AND PETROLOGY OF THE MIGMATITES

In order to characterize the melt behavior in the crust and to gain insight into heat transfer mechanisms, we studied the main structural and petrological features of the El Oro complex migmatites. Metatexites show well-defined leucosome and melanosome layering plus indicators of melt extraction via magma pathways that do

not extend into the overlying metasedimentary rocks (Fig. 2). At the contact with the schlieren migmatites there is an ~100-m-thick transition zone characterized by gradual disruption of the metatexite layering (Riel et al., 2013). This zone is composed of a heterogeneous mixture of metatexite and schlieren migmatite with biotite-rich selvages, leucosome patches, and numerous metasedimentary xenoliths. This is followed by the 7–8-km-thick garnet-bearing schlieren migmatites, which are more homogeneous with numerous quartzitic, aluminous, and layered quartzofeldspathic schollen. The textures of the schlieren migmatites vary from coarse-grained igneous to fine-grained foliated. The foliation has no clear preferred orientation at the scale of the unit and lacks evidence of leucosome-melanosome segregation, magma pathways, or water-flux melting. However, in some outcrops, curved synmigmatitic to late migmatitic foliations are preserved and represent shear zones separating less strained zones of chaotic foliation. In the schlieren migmatitic unit, the metasedimentary xenoliths exhibit a wide range of interesting features ranging from the centimeter to the meter scale (for field photographs, see the Data Repository). Some quartzitic xenoliths are partially molten while others are fractured and filled with leucosome produced in their surroundings. Other aluminous xenoliths are either folded with clear contact with the schlieren migmatites, or partially molten and exhibit a segregated leucosome with respect to the residuum. However, at the rims of these xenoliths, the leucosome becomes diffuse and mixed in the surrounding schlieren migmatite. Evidence of multimeter-scale domal structure made of folded meta-quartzitic xenoliths indicates vertical mass flow within the schlieren migmatitic unit (see Fig. DR4 in the Data Repository).

Another key aspect of the schlieren migmatites concerns their melt content at  $P$ - $T_{\max}$  conditions. As no evidence of water-flux melting, such as an enriched network of leucosome with diffuse contacts and destabilization and consumption of garnet or regions lacking peritectic minerals, has been observed (Weinberg and Hasalová, 2015), we estimated the melt fraction by thermodynamic modeling, using six whole-rock compositions and their related saturating water contents at subsolidus (for details, see the Data Repository). Our results show that, at  $P$ - $T_{\max}$  conditions, the melt content in the schlieren migmatites was 5–15 vol%.

## GEOCHEMISTRY

A typical sample from the schlieren migmatite is heterogeneous, but on average they tend to have 62%–70% silica and a granodiorite composition (Aspden et al., 1995). The metasedimentary rocks show a clear trend in the FeO + MgO versus  $K_2O$  diagram along the line linking quartz + plagioclase to biotite (Fig. 3A). In con-

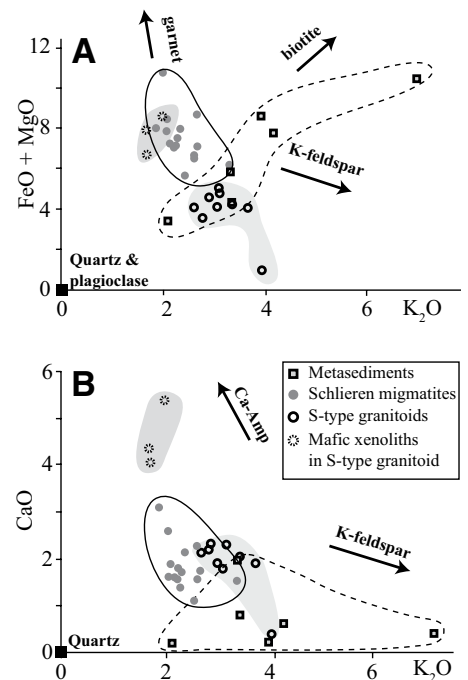


**Figure 3.** Binary plots of selected whole-rock major elements of the El Oro complex (southwestern Ecuador). **A:** FeO + MgO versus  $K_2O$  diagram. **B:** CaO versus  $K_2O$  diagram (Amp—amphibole). For composition data, see the Data Repository (see footnote 1). S-type granitoids are from Aspden et al. (1995). Dashed field marks distribution of metasedimentary rocks; continuous line field marks distribution of schlieren migmatites.

trast, the schlieren migmatites branch out from this trend and define their own trend, pointing toward garnet (Fig. 3A). In the same diagram, S-type granitoids from the belt that intruded further up into the metasedimentary rocks overlap those of the sediments, but define a narrower field. Mafic xenoliths from these granodiorites show enrichment in the ferromagnesian component, plotting together with the schlieren migmatites. Schlieren migmatites show enrichment in CaO (2%–3%) and depletion in  $K_2O$  (2%–3%) compared to the metasedimentary rocks (CaO 0.5%–2% and  $K_2O$  2%–7%), indicating the effect of concentrating garnet (Fig. 3B).

The rare earth element (REE) spectra of the S-type granitoids are similar to that of the leucosome in the metatexite layer (Fig. 4) and are interpreted to be generated by muscovite breakdown. These two spectra plot along the lower values of the field defined by metasedimentary rocks. The schlieren migmatites are interpreted to derive from biotite breakdown, defining a narrow range of REEs that coincides with the mid-values of the field defined by metasediments (Fig. 4). In contrast, the REE spectrum of a segregated leucosome generated by biotite breakdown shows a strong depletion in heavy REEs resulting from extraction of peritectic garnet.

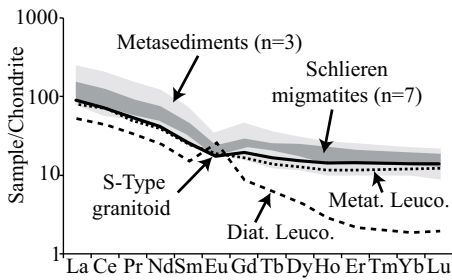


**Figure 4. Whole-rock rare earth element spectra of El Oro complex (southwestern Ecuador) samples normalized to chondrites (Taylor and Gorton, 1977). Color legend as in Figure 1A. Metat.—metatexites; Leuco.—leucosome; Diat.—diatexite.**

## PETROLOGICAL AND GEOCHEMICAL IMPLICATIONS

The schlieren migmatites do not show enrichment of heavy REEs compared to unmelted metasediments (Fig. 4), indicating that melts produced as a result of biotite-dehydration melting reaction were trapped within the rock. This contradicts results in Figure 3, where schlieren migmatites trend toward garnet composition, and can be explained by early removal of  $K_2O$  from the schlieren migmatites by extraction of muscovite-breakdown melt that predated biotite-breakdown melting. The fact that no crosscutting granitic dikes have been observed in the schlieren migmatites or metasedimentary unit supports the conclusion that most melt was trapped in the source. The high CaO content in the biotite + amphibole-bearing S-type granitoids above, south of the migmatite region (Fig. 1B) and its ferromagnesian-rich (amphibole-rich) enclaves, suggest mixing with a CaO-rich mafic magma.

These features suggest that magma that formed as a result of early muscovite breakdown was extracted from the source region during formation of metatexites that are still preserved on top of the schlieren migmatites. Subsequent biotite breakdown gave rise to melt that remained trapped in the source (Fig. 2). Consequently, we interpret the numerous metasedimentary xenoliths in the schlieren migmatitic unit as indicators of a two-step partial melting sequence during increasing temperature conditions.

## THERMAL MODELING

### Numerical Basis

In order to investigate the thermal processes that generated the anatectic gradient in the El Oro complex (Fig. 1C), we used a one-dimensional thermal modeling approach that takes into account temperature-dependent thermal conductivity and capacity (Whittington et al., 2009), radiogenic heat production, latent heat of muscovite and biotite-breakdown melting reactions, melt removal, and parametrized convection with an initial estimate of the likely viscosity

( $10^{12}$ – $10^{16}$  Pa·s). Based on our petrological and geochemical results, the muscovite-breakdown melts are segregated via melt-enhanced fracturing above the melt connectivity threshold, i.e., ~7% (e.g., Rosenberg and Handy, 2005). In the model, this is reflected as heat extracted from the source and emplaced at 5 km depth (corresponding to position of the granitoids in Fig. 1C). In contrast, as supported by the petrological and geochemical evidence, melts produced during biotite-breakdown melting are left in the source.

Our models are set with constant temperature at the surface (20 °C) and with heat flux at the base to get an initial thermal gradient of 25 °C/km. We simulate gabbroic intrusion by imposing a temperature of 1200 °C between 25 and 29 km depth. Subsequently the gabbro cools as it loses heat upward, but temperature is maintained at 29 km depth, the bottom of the model, at 1200 °C for various amounts of time (Fig. 5). Two sets of models have been investigated, purely diffusive (Fig. 5A) or with parameterized convection (Fig. 5B). The  $P$ - $T_{\max}$  estimates of the El Oro complex represent the maximum thermal conditions recorded over the entire duration of the anatectic event (<10 m.y.), but not necessarily at the same moment. In other words, we retrieve the maximum temperature reached at any depth of the models over the modeled period to be able to compare it with the  $P$ - $T_{\max}$  estimates (Fig. 5) (for detailed methodology, see the Data Repository).

## RESULTS

Conductive models indicate that the predicted maximum thermal gradient preserved in the metamorphic record is  $40 \pm 0.4$  °C/km and

slightly concave upward (Fig. 5A). The modeled temperature at the base of the schlieren migmatites is ~950–1100 °C, higher than the  $T_{\max}$  estimate of  $880 \pm 50$  °C. The thickness of the biotite-breakdown melting zone never reaches the observed 7–8 km and the thermal gradient is too high with respect to 15 °C/km estimated in the garnet-bearing migmatites. In contrast, convective models predict lower geothermal gradients, in accord with the metamorphic data (Fig. 5B). The best fit is achieved for a thermal perturbation lasting 3.5 m.y. and a hyperdiffusivity of  $18 \text{ J s}^{-1} \text{ m}^{-1} \text{ K}^{-1}$  (Fig. 5B), corresponding to a shear viscosity for the schlieren migmatites of  $10^{15}$  Pa·s.

## DISCUSSION

The low geothermal gradient in the schlieren migmatites was previously interpreted as the result of thermal buffering due to latent heat of melting (Riel et al., 2013). However, conductive models show that the thermal effect of melt extraction and/or latent heat is low and cannot account for the low geothermal gradient and the width of the melting zone (Fig. 5A). A more efficient heat transfer process is thus required. Models have shown that long-term plutonism can generate low geothermal gradients by continuous melt extraction from the source and transfer to the upper crust (Depine et al., 2008). For similar conditions, Bouilhol et al. (2011) demonstrated that lateral changes of composition are expected due to the formation of pervasive channels via a porosity wave mechanism, which is not observed in the El Oro complex. Therefore, we propose that the main features recorded in the El Oro complex result

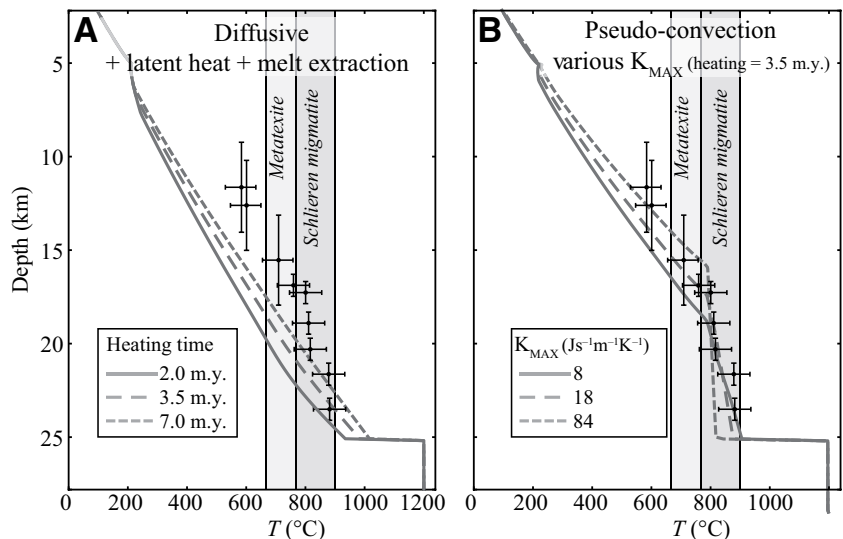


**Figure 5. Thermal modeling results. Diagrams show the maximum temperature ( $T_{\max}$ ) reached at any time during the thermal evolution of the model. A: Diffusive models with latent heat of muscovite and biotite-breakdown melting and extraction of muscovite-breakdown-related melts. B: Pseudoconvective model using a linearly increasing conductivity with respect to melt content during biotite-breakdown melting to a value of  $K_{\max}$  ( $\text{J s}^{-1} \text{ m}^{-1} \text{ K}^{-1}$ ). Higher  $K$  values increase heat transfer across layer and simulated increase in convection vigor. The black crosses represent the pressure- $T_{\max}$  estimates.**

from convection of the schlieren migmatites layer. Convection explains the low geothermal gradient (Fig. 5B), the structural evidence in the form of disorganized, chaotic flow of the schlieren migmatites, and geochemical data (Figs. 3 and 4) indicating that melts produced by biotite-dehydration melting reaction were not extracted from the source.

Using the critical Rayleigh number for an infinite fluid between two free surfaces, we estimate that to allow for convection, the viscosity of the schlieren migmatites has to be  $<7 \times 10^{17}$  Pa·s across the 7-km-thick schlieren migmatites (assuming a  $T$  difference of 100 °C across the layer). Burg and Vigneresse (2002) showed that, for a partially molten metapelite containing 0%–60% melt, the shear viscosity drops from  $10^{18}$  Pa·s at 600 °C to  $10^6$  Pa·s at 900 °C. Hashim et al. (2013) estimated a viscosity of  $10^{11}$ – $10^{12}$  Pa·s for partially molten metapelite with 20%–25% of melt at 825 °C. Given that in the El Oro complex the schlieren migmatites contained 5%–15% melt, we infer an effective viscosity of  $10^{12}$ – $10^{16}$  Pa·s. These values are lower than the estimated critical viscosity and are consistent with our convection model (Fig. 2).

How did the melts produced during biotite-breakdown melting remain trapped in the rock? Because the melt fraction estimated in the schlieren migmatites at  $P$ - $T_{\max}$  conditions is relatively low (5%–15%), a possible explanation can be a combination of (1) a drop of solid cohesion, leading to melt-accommodated grain boundary sliding or granular flow that opposes melt segregation (Walte et al., 2005); (2) a low-density contrast between melt and host rock resulting from a melting reaction with insignificant volume change (Rushmer, 2001); (3) the high viscosity of silicic melts; and (4) biotite flake aggregates leading to a very low permeability normal to the layering and acting as a barrier against melt segregation (Laporte and Watson, 1995). Our thermodynamic modeling indicates that the schlieren migmatites contained  $10\% \pm 5\%$  of biotite at  $P$ - $T_{\max}$  conditions (see the Data Repository). Therefore, residual aggregates of biotite (schlieren) and granular flow due to loss of solid cohesion are likely to play an important role, preventing melt transfer out of the convective cells. Further studies are required to fully understand this melt behavior during biotite-breakdown melting.

## CONCLUSIONS

Thermal models of the Triassic anatectic rocks in the El Oro complex show that crustal-scale mass convection is an efficient heat

transfer process that can lead to the observed low geothermal gradient across a wide layer of schlieren migmatites. Based on structural and metamorphic data and modeling, we propose that in the schlieren migmatites layer that formed at the base of the biotite-rich metasedimentary sequence, convection may have been the main heat transfer process at temperatures ranging from 780 to 900 °C. This study provides new insights into the complex dynamics of partially molten felsic crust and proposes a new mechanism to account for observed low geothermal gradients and long-lived partially molten middle to lower crust, such as beneath large orogenic plateaus.

## ACKNOWLEDGMENTS

This research was funded by the Structure, Evolution et Dynamique de l'Intérieur de la Terre (SEdit) program (Institut National des Sciences de l'Univers, France, 2008–2009) and by the European Research Council (ERC StG 279828). We thank Stéphane Guillot, Etienne Jaillard, Jean Braun, Nicolas Walte, and three anonymous reviewers who contributed to greatly improve the paper.

## REFERENCES CITED

- Aspden, J.A., Bonilla, W., and Duque, P., 1995, The El Oro metamorphic complex, Ecuador: Geology and economic mineral deposits: *Overseas Geology and Mineral Resources Issue 67*: Nottingham, British Geological Survey Publication, 67 p.
- Bittner, D., and Schmeling, H., 1995, Numerical modeling of melting processes and induced diapirism in the lower crust: *Geophysical Journal International*, v. 123, p. 59–70, doi:10.1111/j.1365-246X.1995.tb06661.x.
- Bouilhoul, P., Connolly, J.A.D., and Burg, J.-P., 2011, Geological evidence and modeling of melt migration by porosity waves in the sub-arc mantle of Kohistan (Pakistan): *Geology*, v. 39, p. 1091–1094, doi:10.1130/G32219.1.
- Burg, J.P., and Vigneresse, J.L., 2002, Non-linear feedback loops in the rheology of cooling-crystallizing felsic magma and heating-melting felsic rock, in De Meer, S., et al., eds., *Deformation mechanisms, rheology and tectonics: Current status and future perspectives*: Geological Society of London Special Publication 200, p. 275–292, doi:10.1144/GSL.SP.2001.200.01.16.
- Caldwell, W.B., Klemperer, S.L., Rai, S.S., and Lawrence, J.F., 2009, Partial melt in the upper-middle crust of the northwest Himalaya revealed by Rayleigh wave dispersion: *Tectonophysics*, v. 477, p. 58–65, doi:10.1016/j.tecto.2009.01.013.
- Depine, G.V., Andronicos, C.L., and Phipps-Morgan, J., 2008, Near-isothermal conditions in the middle and lower crust induced by melt migration: *Nature*, v. 452, p. 80–83, doi:10.1038/nature06689.
- Ding, L., Kapp, P., Yuey, Y., and Lai, Q., 2007, Post-collisional calc-alkaline lavas and xenoliths from the southern Qiangtang terrane, central Tibet: *Earth and Planetary Science Letters*, v. 254, p. 28–38, doi:10.1016/j.epsl.2006.11.019.
- Gabriele, P., 2002, HP terranes exhumation in an active margin setting: *Geology, petrology and geochemistry of the Raspas Complex in SW Ecuador* [Ph.D. thesis]: Lausanne, Switzerland, University of Lausanne, 258 p.
- Hashim, L., Gaillard, F., Champallier, R., Le Breton, N., Arbaret, L., and Scaillot, B., 2013, Experimental assessment of the relationships between electrical resistivity, crustal melting and strain localization beneath the Himalayan-Tibetan belt: *Earth and Planetary Science Letters*, v. 373, p. 20–30, doi:10.1016/j.epsl.2013.04.026.
- Laporte, D., and Watson, E.B., 1995, Experimental and theoretical constraints on melt distribution in crustal sources: The effect of crystalline anisotropy on melt interconnectivity: *Chemical Geology*, v. 124, p. 161–184, doi:10.1016/0009-2541(95)00052-N.
- Mahéo, G., Blichert-Toft, J., Pin, C., Guillot, S., and Pêcher, A., 2009, Neogene partial melting of contrasted mantle and crustal sources beneath the south Asian margin (south Karakorum, Pakistan): Implications for the late-stage geodynamic evolution of the India-Asia convergence zone: *Journal of Petrology*, v. 50, p. 427–449, doi:10.1093/petrology/egp006.
- Riel, N., et al., 2013, A metamorphic and geochronological study of the Triassic El Oro metamorphic Complex in Ecuador: Implications for high-temperature metamorphism in a forearc zone: *Lithos*, v. 156, p. 41–68, doi:10.1016/j.lithos.2012.10.005.
- Rosenberg, C.L., and Handy, M.R., 2005, Experimental deformation of partially melted granite revisited: Implications for the continental crust: *Journal of Metamorphic Geology*, v. 23, p. 19–28, doi:10.1111/j.1525-1314.2005.00555.x.
- Rushmer, T., 2001, Volume change during partial melting reactions: Implications for melt extraction, melt geochemistry and crustal rheology: *Tectonophysics*, v. 342, p. 389–405, doi:10.1016/S0040-1951(01)00172-X.
- Taylor, S.R., and Gorton, M.P., 1977, Geochemical application of spark source mass spectrography—III. Element sensitivity, precision and accuracy: *Geochimica et Cosmochimica Acta*, v. 41, p. 1375–1380, doi:10.1016/0016-7037(77)90080-1.
- Walte, N.P., Bons, P.D., and Passchier, C.W., 2005, Deformation of melt-bearing systems: Insight from in situ grain-scale analogue experiments: *Journal of Structural Geology*, v. 27, p. 1666–1679, doi:10.1016/j.jsg.2005.05.006.
- Weinberg, R.F., and Hasalová, P., 2015, Water-fluxed melting of the continental crust: A review: *Lithos*, v. 212–215, p. 158–188, doi:10.1016/j.lithos.2014.08.021.
- Whittington, A.G., Hofmeister, A.M., and Nabelek, P.L., 2009, Temperature-dependent thermal diffusivity of the Earth's crust and implications for magmatism: *Nature*, v. 458, p. 319–321, doi:10.1038/nature07818.
- Yuan, X., Sobolev, S.V., Kind, R., and Oncken, O., and the Andes Seismology Group, 2000, Subduction and collision processes in the central Andes constrained by converted seismic phases: *Nature*, v. 408, p. 958–961, doi:10.1038/35050073.

Manuscript received 29 July 2015

Revised manuscript received 23 October 2015

Manuscript accepted 1 November 2015

Printed in USA



## Geology

### Convection in a partially molten metasedimentary crust? Insights from the El Oro complex (Ecuador)

Nicolas Riel, Jonathan Mercier and Roberto Weinberg

*Geology* published online 20 November 2015;  
doi: 10.1130/G37208.1

---

**Email alerting services**

click [www.gsapubs.org/cgi/alerts](http://www.gsapubs.org/cgi/alerts) to receive free e-mail alerts when new articles cite this article

**Subscribe**

click [www.gsapubs.org/subscriptions/](http://www.gsapubs.org/subscriptions/) to subscribe to *Geology*

**Permission request**

click <http://www.geosociety.org/pubs/copyrt.htm#gsa> to contact GSA

Copyright not claimed on content prepared wholly by U.S. government employees within scope of their employment. Individual scientists are hereby granted permission, without fees or further requests to GSA, to use a single figure, a single table, and/or a brief paragraph of text in subsequent works and to make unlimited copies of items in GSA's journals for noncommercial use in classrooms to further education and science. This file may not be posted to any Web site, but authors may post the abstracts only of their articles on their own or their organization's Web site providing the posting includes a reference to the article's full citation. GSA provides this and other forums for the presentation of diverse opinions and positions by scientists worldwide, regardless of their race, citizenship, gender, religion, or political viewpoint. Opinions presented in this publication do not reflect official positions of the Society.

---

**Notes**

---

Advance online articles have been peer reviewed and accepted for publication but have not yet appeared in the paper journal (edited, typeset versions may be posted when available prior to final publication). Advance online articles are citable and establish publication priority; they are indexed by GeoRef from initial publication. Citations to Advance online articles must include the digital object identifier (DOIs) and date of initial publication.

---